Table 4
Optional organ weights including the liver, adrenal, and kidney in antagonistic version

Lab	Body weights/organ weights	Substances								
		V.C.	TP	F	G	I	C	K	D	H
1	Starting body wt. (g)	216.2 ± 10.9	216.1 ± 8.8	214.9 ± 10.6	216.6 ± 10.8	218.1 ± 12.5	216.5 ± 8.1	216.0 ± 8.2	219.4 ± 11.3	215.2 ± 9.7
	Terminal body wt. (g)	260.0 ± 17.4	267.4 ± 16.5	263.3 ± 17.8	272.2 ± 9.5	248.7 ± 17.1	266.3 ± 11.7	245.7 ± 11.1*	263.6 ± 11.8	261.5 ± 12.5
	Liver (g)	10.0 ± 1.0	10.4 ± 0.9	11.3 ± 1.3	10.9 ± 0.9	17.3 ± 1.2*	12.5 ± 0.8*	9.6 ± 0.8	10.4 ± 0.5	10.0 ± 0.8
2	Starting body wt. (g)	256.8 ± 11.0	258.9 ± 9.2	259.3 ± 11.6	257.6 ± 10.9	256.8 ± 9.6	258.9 ± 10.8	258.0 ± 10.6	258.9 ± 10.7	255.4 ± 12.7
	Terminal body wt. (g)	313.2 ± 14.7*	331.9 ± 14.3	326.1 ± 16.4	332.2 ± 20.7	270.8 ± 44.6*	329.8 ± 18.7	309.5 ± 13.9*	335.3 ± 15.6	327.4 ± 23.1
	Liver (g)	13.8 ± 0.7	15.6 ± 2.1	15.8 ± 2.3	15.1 ± 0.9	22.8 ± 3.6*	17.7 ± 1.7	14.1 ± 0.8	15.6 ± 1.4	15.1 ± 2.2
3	Starting body wt. (g)	254.1 ± 13.8	254.4 ± 13.6	255.1 ± 12.3	255.1 ± 12.4	255.6 ± 13.1	255.3 ± 14.7	255.2 ± 14.9	254.3 ± 15.9	254.6 ± 16.6
	Terminal body wt. (g)	303.3 ± 16.4	314.7 ± 20.9	307.0 ± 24.0	317.5 ± 10.9	248.1 ± 62.4*	322.7 ± 23.5	292.7 ± 18.1	310.6 ± 23.1	313.2 ± 24.2
	Liver (g)	12.9 ± 1.2	13.7 ± 1.7	14.2 ± 1.7	13.7 ± 0.5	18.6 ± 2.5*	16.0 ± 1.3	13.0 ± 0.9	12.8 ± 1.4	13.5 ± 2.5
	Adrenals (mg)	57.0 ± 10.8	49.5 ± 8.3	54.3 ± 12.5	58.0 ± 5.9	55.5 ± 3.6	56.6 ± 3.5	63.2 ± 7.0*	56.5 ± 7.8	55.5 ± 7.7
	Kidneys (mg)	2106 ± 212	2207 ± 228	2316 ± 273	2342 ± 34	2152 ± 216	2329 ± 197	2236 ± 132	2184 ± 198	2195 ± 201

V.C., vehicle control; TP, testosterone propionate. Each substance was coadministered with 0.2 mg/kg TP. $n = 6$ rats/group/Lab.
* Significantly different from TP group at $P < 0.05$.

LABC weight in rats given G plus TP was significantly lower than that in the TP group in Lab 2, the normalized change of this organ was not so apparent. The total of the five accessory sex organ weights in rats given I plus TP and K plus TP was lower than in rats given TP in all laboratories. The seminal vesicle weight changes in rats given I plus TP and K plus TP were most sensitive among the five organs (Fig. 2).

4. Discussion

Japanese laboratories performed the validation studies of Phase 2 using methyltestosterone, vinclozolin, and *p,p'*-DDE as a part of the national validation program with the result that the Hershberger assay proposed by the OECD was suggested to be a good screening assay to detect androgen agonistic and antagonistic effects (Yamasaki et al., 2003a).

We also performed the Hershberger assay using coded chemicals as part of a national validation Phase 3 as the next step for the OECD guideline process of this assay. The weights of all the accessory sex organs from the experimental animals in all the laboratories exhibited significantly the same changes in the agonistic version; almost all organ weights increased in the rats given coded substance L, and no organ showed any response in rats given coded substances A and B. We received the information from the coordinator of this validation study after all tests were finished that a group of L and E was the same compound and a dose of L was higher than that of E, and that A and B were reported to have no agonistic properties and L and E were a weak agonistic compound. In addition, the normalized weights of all the tissues treated with coded substances in each assay fell within narrow ranges. Therefore, we think that the Hershberger assay is a good screening assay for detecting the androgen agonistic effects of chemicals. The findings that the terminal body weights in rats given coded L were depressed in all laboratories and no body weight changes were detected in rats given coded substance E in all laboratories means that a dose of L was a toxic level and a dose of E had no observed effect. The androgen agonistic effects were detected by the administration of toxic level in this study, but weak agonistic and antagonistic properties of some weak chemicals were detected when non-toxic level doses were administered (Yamasaki et al., 2003a,b).

In the antagonistic version, almost all the sex accessory organs decreased in rats given coded substances I plus TP and K plus TP in all laboratories compared with each organ weight in the rats given TP only, and some organ weights also decreased in the coded substance C

Table 5
Mean body weights and mean organ weights in antagonistic version

Lab	Body weights/organ weights	Chemicals								
		V.C.	TP	F	G	I	C	K	D	H
1	Terminal body wt. (g)	260.0 ± 17.4	267.4 ± 16.5	263.3 ± 17.8	272.2 ± 9.5	248.7 ± 17.1	266.3 ± 11.7	245.7 ± 11.1*	263.6 ± 11.8	261.5 ± 12.5
	Ventral prostate (mg)	14.4 ± 1.5*	102.4 ± 17.6	82.0 ± 7.7	85.9 ± 19.3	28.3 ± 5.9*	78.9 ± 14.6*	41.4 ± 5.9*	80.6 ± 10.7*	24.9 ± 3.6*
	Seminal vesicles (mg)	23.8 ± 3.1*	194.8 ± 38.9	191.4 ± 40.0	185.7 ± 33.5	35.5 ± 6.2*	144.5 ± 29.1	60.6 ± 8.2*	154.7 ± 32.5	28.2 ± 3.8*
	LABC (mg)	119.0 ± 7.0*	306.2 ± 39.1	307.8 ± 40.0	302.3 ± 29.4	125.7 ± 13.4*	280.7 ± 29.7	155.8 ± 21.8*	302.9 ± 40.4	148.3 ± 18.6*
	Glans penis (mg)	29.4 ± 2.9*	60.9 ± 5.3	61.9 ± 5.5	61.2 ± 2.1	32.0 ± 3.9*	53.6 ± 3.3*	41.7 ± 6.4*	64.5 ± 6.1	30.3 ± 4.2*
	Cowper's glands (mg)	3.2 ± 1.3*	18.4 ± 4.6	20.1 ± 1.7	16.2 ± 3.5	4.9 ± 0.8*	16.4 ± 1.9	8.3 ± 1.8*	18.1 ± 3.3	4.7 ± 1.3*
	Total of five organs (mg)	189.9 ± 10.6*	682.7 ± 85.8	663.2 ± 81.3	651.2 ± 65.6	226.5 ± 20.6*	573.9 ± 62.2	307.7 ± 25.4*	620.8 ± 74.6	236.3 ± 24.2*
2	Terminal body wt. (g)	313.2 ± 14.7*	331.9 ± 14.3	326.1 ± 16.4	332.2 ± 20.7	270.8 ± 44.6*	329.8 ± 18.7	309.5 ± 13.9*	335.3 ± 15.6	327.4 ± 23.1
	Ventral prostate (mg)	17.7 ± 2.7*	144.9 ± 19.4	135.0 ± 12.9	129.0 ± 31.5	28.0 ± 8.9*	126.5 ± 40.0	61.6 ± 25.7*	115.5 ± 26.3	28.2 ± 8.9*
	Seminal vesicles (mg)	47.5 ± 8.4*	463.2 ± 70.1	405.9 ± 69.8	439.7 ± 68.7	77.8 ± 26.4*	352.5 ± 80.3*	177.7 ± 43.8*	357.1 ± 40.3*	65.9 ± 11.2*
	LABC (mg)	217.7 ± 25.2*	575.3 ± 31.8	539.6 ± 53.0	529.9 ± 32.2*	218.1 ± 39.6*	496.4 ± 71.6*	336.0 ± 46.3*	532.4 ± 56.5	235.9 ± 29.0*
	Glans penis (mg)	49.9 ± 2.9*	73.0 ± 3.7	75.6 ± 5.9	75.2 ± 2.1	49.8 ± 1.7*	71.7 ± 2.5	63.9 ± 6.2*	73.0 ± 3.3	49.7 ± 2.0*
	Cowper's glands (mg)	5.7 ± 0.9*	33.0 ± 5.4	28.5 ± 5.6	31.0 ± 2.6	10.5 ± 3.8*	30.9 ± 6.5	22.9 ± 9.1	25.7 ± 6.2	10.4 ± 3.4*
	Total of five organs (mg)	338.4 ± 29.0*	1290.2 ± 111.4	1184.6 ± 97.1	1204.6 ± 115.7	384.2 ± 71.6*	1078.0 ± 174.3*	662.0 ± 111.1*	1103.7 ± 89.4*	390.0 ± 29.6*
3	Terminal body wt. (g)	303.3 ± 16.4	314.7 ± 20.9	307.0 ± 24.0	317.5 ± 10.9	248.1 ± 62.4	322.7 ± 23.5	292.7 ± 18.1	310.6 ± 23.1	313.2 ± 24.2
	Ventral prostate (mg)	20.7 ± 3.5*	159.1 ± 31.2	142.0 ± 34.5	132.8 ± 20.1	36.2 ± 9.4*	107.2 ± 17.8*	67.8 ± 24.5*	133.6 ± 24.2	39.8 ± 5.2*
	Seminal vesicles (mg)	53.9 ± 5.2*	459.7 ± 97.2	437.1 ± 120.5	411.6 ± 59.7	73.9 ± 7.9*	323.7 ± 59.0	159.6 ± 45.0*	317.1 ± 62.3*	76.3 ± 10.8*
	LABC (mg)	193.1 ± 11.3*	518.1 ± 74.2	460.2 ± 84.7	494.4 ± 50.1	165.4 ± 35.5*	396.4 ± 50.9*	262.6 ± 47.8*	452.4 ± 64.2	221.8 ± 51.5*
	Glans penis (mg)	50.9 ± 3.8*	93.5 ± 4.6	86.3 ± 7.9	89.6 ± 7.6	60.2 ± 7.3*	83.9 ± 4.3	73.2 ± 10.0*	90.2 ± 6.1	60.8 ± 3.4*
	Cowper's glands (mg)	8.3 ± 2.8*	35.6 ± 6.5	37.5 ± 11.1	33.4 ± 5.3	9.3 ± 2.5*	23.5 ± 5.9*	20.9 ± 4.6*	34.8 ± 6.7	12.0 ± 3.8*
	Total of five organs (mg)	326.9 ± 21.3*	1266.0 ± 151.6	1163.1 ± 217.1	1161.6 ± 84.1	345.0 ± 57.2*	934.7 ± 130.1*	584.2 ± 90.7*	1028.0 ± 110.7*	410.7 ± 61.4*

V.C., vehicle control; TP, testosterone propionate. Each substance was coadministered with 0.2 mg/kg TP. $n = 6$ rats/group/Lab.
* Significantly different from TP group at $P < 0.05$.

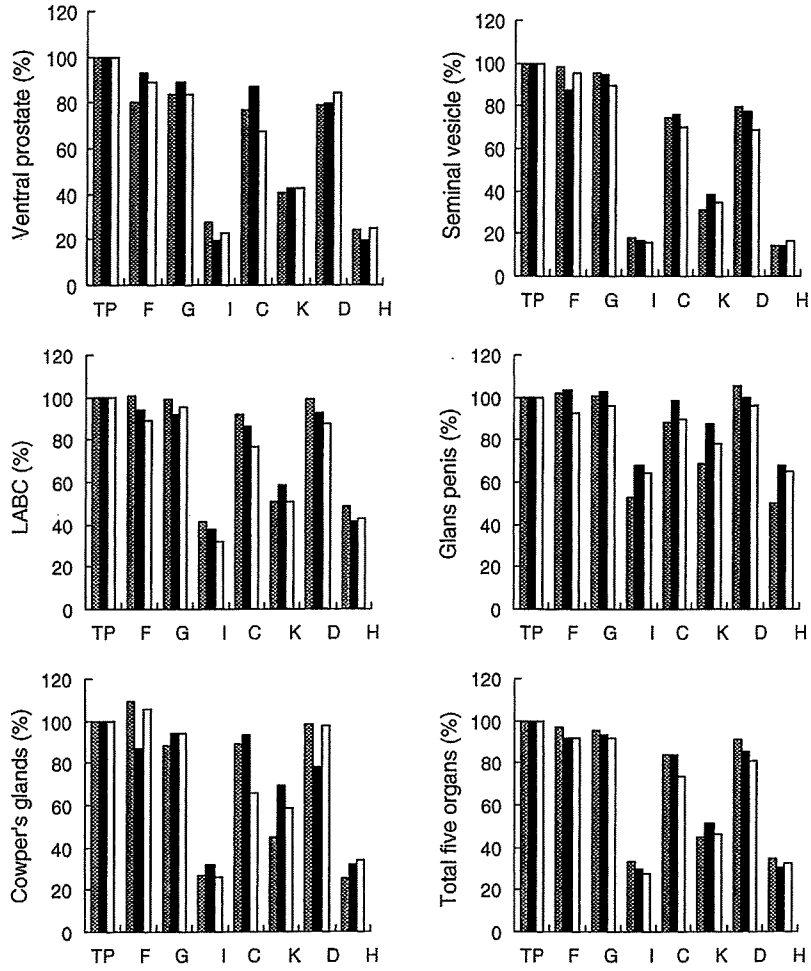

Fig. 2. Organ weights in antagonistic version. Values from each laboratory were normalized to the value of TP group set equal to 100%. LABC: levator ani and bulbocavernosus muscle; F, G, I, C, K, D, and H: coded chemicals; TP: testosterone propionate. $n = 6$ rats/group/Lab (▩, Lab 1; ■, Lab 2; □, Lab 3).

plus TP and D plus TP groups. No changes were detected in rats given coded substances F and G. These findings demonstrate that coded substances I, C, K, and D had antagonistic properties and coded substances F and G had no antagonistic properties. We accepted the information; substances F and G were negative compounds, I, C, K, and D were weak antagonistic compounds, and H was a positive control compound, flutamide; the groups of substances I and C, or K and D were the same compound, and dose levels of I and K were higher than those of C and D. We also received the information that C and I were *p,p'*-DDE and D and K were linurone. The ventral prostate and glans penis in Lab 1, the seminal vesicle and LABC in Lab 2, and the ventral prostate, LABC and Cowper's glans in Lab 3 were significantly affected in the rats given coded substance C plus TP. In addition, the ventral prostate in Lab 1 and seminal vesicle in Labs 2 and 3 were significantly affected in rats given coded substance D plus TP. The differential effects across laboratories were observed in rats given coded C plus TP and D plus TP. We found that the most sensitive organ among the five accessory sex organs was the prostate and/or seminal vesicle in our previous validation Phase 2 study, and in the Hershberger assays using various chemicals (Yamasaki et al., 2003a,b). The ventral prostate and/or seminal vesicle were responded with or without significant differences in rats given coded substances C plus TP and D plus TP, so we determined that coded C and D have androgen antagonistic properties. On the other hand, the LABC weight in rats given coded substance G plus TP was significantly lower than that in the TP group in Lab 2, but the normalized change of this organ was not so apparent. Therefore, the Japanese data in this study demonstrated that the Hershberger assay

is considered to be a good screening assay for detecting the androgen antagonistic effects of chemicals. The findings that some animals died in rats given coded substance I and decreased body weights were detected in rats given K and I, and the liver weights increased in rats given I means the coded substances I and K were at a toxic dose level. In addition, the liver weights increased in rats given C in one laboratory, so a dose of C may be at a toxic level. The general toxicity is considered to be important for this assay, because a 10% change in terminal weight is suggested to affect some Hershberger assay endpoints (Marty et al., 2003).

In conclusion, we performed the OECD validation study Phase 3 using coded chemicals. All five accessory sex organs responded with statistically significant changes in weight within a narrow window in the agonistic and antagonistic versions, and no false positive or false negative results were observed in this study. Therefore, the Japanese studies support the Hershberger assay as a reliable and reproducible screening assay for the detection of androgen agonistic and antagonistic effects.

Acknowledgments

This study was supported by the grant by the Ministry of Economy, Trade and Industry, the Ministry of Health, Labour and Welfare, and Ministry of the Environment in Japan.

References

Bülbring, E., Burn, J.H., 1935. The estimation of oestrin and of male hormone in oily solution. J. Physiol. 85, 320–333.

Deanesly, R., Parkes, A.S., 1936. Comparative activities of compounds of the androsterone-testosterone series. Biochem. J. 30, 291–303.

Di Salle, E., Briatico, G., Giudici, D., Ornati, G., Panzeri, A., 1994. Endocrine properties of the testosterone 5α-reductase inhibitor turosteride (FCE 26073). J. Steroid Biochem. Mol. Biol. 48, 241–248.

Dingemanse, E., Frued, J., Laquer, E., 1935. Differences between male hormone extracts from urine and from testes. Nature 135, 184.

Eisenberg, E., Gordan, G.S., 1950. The levator ani muscle of the rat as an index of mytrophic activity of steroidal hormones. J. Pharmacol. Exp. Therap. 99, 38–44.

Eisenberg, E., Gordan, G.S., Elliott, H.W., 1949. Testosterone and tissue respiration of the castrate male rat with a possible test for mytrophic activity. Endocrinology 45, 113–119.

Hershberger, L.G., Shipley, E.G., Meyer, R.K., 1953. Myotrophic activity of 19-nortestosterone and other steroids determined by modified levator ani muscle method. Proc. Soc. Exp. Biol. Med. 83, 175–180.

Korenchevsky, V., 1932. The assay of testicular hormone preparations. Biochem. J. 26, 413–422.

Korenchevsky, V., Dennison, M., Schalit, R., 1932. The response of castrated male rats to the injection of the testicular hormone. Biochem. J. 26, 1306–1314.

Korenchevsky, V., Dennison, M., Kohn-Speyer, A., 1933a. Changes produced by testicular hormone in normal and in castrated rats. Biochem. J. 27, 557–579.

Korenchevsky, V., Dennison, M., Kohn-Speyer, A., 1933b. On the assay and the absorption of testicular hormone dissolved in oil. Biochem. J. 27, 778–782.

Marty, M.S., Johnson, K.A., Carney, E.W., 2003. Effect of feed restriction on Hershberger and pubertal male assay endpoints. Birth Defects Res. (Part B) 68, 363–374.

McLachlan, J.A., 1993. Functional toxicology: a new approach to detect functionally active xenobiotics. Environ. Health Perspect. 101, 386–387.

McLachlan, J.A., Korach, K.S., 1995. Estrogens in the environment global health implications. Environ. Health Perspect. 103 (Suppl. 7), 3–4.

Organisation for Economic Cooperation and Development (OECD), 1998. Report of the first meeting of the OECD endocrine disrupter testing and assessment (EDTA) working group.

Organisation for Economic Cooperation and Development (OECD), 2000. The second meeting of the OECD validation management group (VMG) for the screening and testing of endocrine disrupters.

Organisation for Economic Cooperation and Development (OECD), 2002. Final OECD report of the work towards the validation of the rat Hershberger assay: Phase 1, androgenic response of testosterone propionate, and anti-androgenic effects of flutamide. Task force on endocrine disrupters testing and assessment (EDTA) of the test guidelines program.

Organisation for Economic Cooperation and Development (OECD), 2003. The fourth meeting of the OECD validation management group (VMG) for the screening and testing of endocrine disrupters.

Peets, E.A., Henson, M.F., Neri, R., 1973. On the mechanism of the anti-androgenic action of flutamide (α-α-α-trifluoro-2-methyl-4′-nitro-m-propionotoluidide) in the rat. Endocrinology 94, 532–540.

Raynaud, J.P., Bouton, M.M., Moguilewsky, M., Ojasoo, T., Philibert, D., Beck, G., Labrie, F., Mornon, J.P., 1980. Steroid hormone receptors and pharmacology. J. Steroid Biochem. 12, 143–157.

Raynaud, J.P., Bonne, C., Moguilewsky, M., Lefebvre, F.A., Bélanger, A., Labrie, F., 1984. The pure anti-androgen RU 23908 (Anandron®), a candidate of choice for the combined anti-hormonal treatment of prostatic cancer: a review. Prostate 5, 299–311.

USEPA, 1998. Endocrine Disruptor Screening and Testing Advisory Committee (EDSTAC) final report. EPA/743/R-98/003.

Wainman, P., Shipounoff, G.C., 1941. The effects of castration and testosterone propionate on the striated perineal musculature in the rat. Endocrinology 29, 975–978.

Wakeling, A., Furr, B.J.A., Glen, A.T., Hughes, L.R., 1981. Receptor binding and biological activity of steroidal and non-steroidal anti-androgens. J. Steroid Biochem. 15, 355–359.

Yamasaki, K., Sawaki, M., Ohta, R., Okuda, H., Katayama, S., Yamada, T., Ohta, T., Kosaka, T., Owens, W., 2003a. OECD validation of the Hershberger assay in Japan: Phase 2-Dose response of methyltestosterone, vinclozolin and *p,p′*-DDE. Environ. Health Perspect. 111, 1912–1919.

Yamasaki, K., Takeyoshi, M., Yakabe, Y., Sawaki, M., Imatanaka, M., Shinoda, K., Takatsuki, M., 2003b. Immature rat uterotrophic assay of 18 chemicals and Hershberger assay of 30 chemicals. Toxicology 183, 95–115.

秦野研究所年報
27, 28-35 (2004)

マウスを用いる子宮肥大試験

太田　亮[1]，田面喜之[2]，宮原　敬[2]，丸茂秀樹[1]

The Mouse Uterotrophic Assay

Ryo Ohta[1], Yoshiyuki Tazura[2], Takashi Miyahara[2], Hideki Marumo[1]

The mouse uterotrophic assay was attempted in ovariectomized mice using ethinyl estradiol as a reference compound and the result was comparable with the rat uterotrophic assay. Ovariectomized mice were exposed to bisphenol A and twenty other selected chemicals by gavage or subcutaneous injection according to the protocol drafted by the OECD Validation Management Group for the Screening. The results demonstrated that bisphenol A had potency not only of estrogenicity but also of anti-estrogenicity, and that ten of the twenty chemicals revealed either estrogenic or anti-estrogenic activity on the uterus of mice. These results support the mouse uterotrophic assay as a useful screening method for detection of estrogenic and anti-estrogenic compounds.

緒言

子宮肥大試験（Uterotrophic assay）は，エストロゲン活性を調べるための*in vivo*試験系として，1930年代から用いられてきた古い手法であるが，現在は，内分泌かく乱化学物質のスクリーニング試験法としての応用が期待され，OECDなどが中心となって，その有用性を確認する作業（バリデーション作業）が国際レベルで進められている[1-3]．OECDが提唱している子宮肥大試験のガイドライン案では，「囓歯類を用いる子宮肥大試験」となっているが，これまで実施されてきたOECDバリデーション作業は，ラットのみである[1-3]．一方，同じ囓歯類でもマウスはこれまで子宮肥大試験に使用されてこなかったが，マウスはラットに比べて体が小さく，子宮も著しく軽量なため，重量測定の前処理などに熟練を要することや，測定値に正確性を欠くことなどが敬遠される主な理由と考えられる．しかしながら，マウスには，被験物質量がラットの約1/10で済むことや，飼育スペースが節約できること，遺伝子発現変化に関する情報が多いことなど利点も多く，将来，マウスが子宮肥大試験に使用される可能性は高いと考えられる．そこで，本稿では，マウスを用いる子宮肥大試験の検証を目的として，エチニルエストラジオール（EE）投与による子宮重量増加をマウス－ラット間で比較した結果と，ビスフェノールA（BPA），さらには，エストロゲン様作用が疑われている種々の化学物質について実施したマウス子宮肥大試験の結果を紹介する．

材料および方法

実験1．EE投与による子宮重量増加の用量反応性

実験は，OECDバリデーション作業のプロトコール案[1]に準拠して，幼若マウスを用いる3日間経口投与法，幼若マウスを用いる3日間皮下投与法，卵巣摘出マウスを用いる7日間経口投与法および卵巣摘出マウスを用いる7日間皮下投与法の4種類を実施した．動物は，ICR系雌マウス（日本チャールス・リバー，横浜）を用い，本館飼育室内で，ペパークリーン（日本エスエルシー，浜松）を入れたTPX樹脂製ケージに収容し，固型飼料（CE-2，日本クレア，東京）および水道水を自由摂取させて飼育した．EE（純度99.0％，和光純薬工業，大阪）は，少量のエタノールに溶解後，コーン油で所定の濃度に調製して，投与した．EEの投与量は，幼若マウスの経

1 Safety Testing Laboratory
2 Animal Husbandry Unit

口投与法では0.3～150 μg/kg/day，皮下投与法では0.1～50 μg/kg/day，卵巣摘出マウスの経口投与法では0.3～100 μg/kg/day，皮下投与法では0.03～10 μg/kg/dayの範囲に設定し，対照群の動物にはコーン油のみを投与した．投与は，幼若マウスの場合は哺育19日から，卵巣摘出マウスの場合は8週齢から開始し，1群当たりの例数は5～6とした．投与した動物は，最終投与の約24時間後に頚椎脱臼し，速やかに放血致死させた．その際，子宮は膣とともに摘出し，実体顕微鏡下で脂肪を除去した後，膣を子宮頚の外子宮口の位置で切り離した．子宮重量は，子宮内液を含んだ状態でまず測定し（wet weight），次に子宮壁の一部を切開し，子宮内液をガーゼで吸い取った後，再度，重量を測定した（blotted weight）．得られたデータは一元配置の分散分析で解析し，有意性が認められた場合には，対照群を基準群としてDunnettの多重比較検定を行った．なお，本稿ではblotted weightのみを指標とした．

実験2．BPAの卵巣摘出マウスを用いた子宮肥大試験

実験は，OECDバリデーションプロトコール案[1]の卵巣摘出動物を用いる7日間皮下投与法に準拠して行い，エストロゲン作用と抗エストロゲン作用を調べた．動物は，6週齢で卵巣を摘出したC57BL/6J系マウス（日本エスエルシー）を動物繁殖研究所（茨城）から入手し，膣スメアで性周期が回帰していないことを確認した後，8週齢で試験に供した．動物の飼育条件は，実験1と同様にした．BPA（純度99.0％，和光純薬工業）は，メノウ乳鉢で破砕後，少量のエタノールに溶解し，コーン油で調製した．EEは，実験1と同様に調製した．群構成は，表1に従い，BPAの投与量は10～300 mg/kg/dayの範囲に設定した．陰性対照群の動物には，コーン油を皮下投与した．陽性対照群の動物には，実験1の結果のED_{10}～ED_{20}に相当する0.2 μg/kg/dayのEEを皮下投与し，抗エストロゲン作用を調べる試験系では，ED_{60}～ED_{70}に相当する0.6 μg/kg/dayのEEを併用皮下投与した．1群当たりの匹数は6とした．子宮重量の測定およびデータの解析は，実験1と同様にした．ただし，陽性対照群と陰性対照群の比較については，Studentのt検定を用いた．

実験3．化学物質の卵巣摘出マウスを用いた子宮肥大試験

実験は，OECDバリデーションプロトコール案[1]に準拠して，卵巣摘出マウスを用いる7日間経口投与法と卵巣摘出マウスを用いる7日間皮下投与法で行った．動物の系統，飼育条件等は，実験2と同様にした．実験に供した化学物質は，以

表1　群構成

Evaluation / Group	Estrogenic action	Anti−estrogenic action
Negative control	Vehicle	Vehicle plus EE [b)]
Low dose	Test substance	Test substance plus EE [b)]
Medium low dose	Test substance	Test substance plus EE [b)]
Medium high dose	Test substance	Test substance plus EE [b)]
High dose	Test substance	Test substance plus EE [b)]
Positive control	EE [a)]	Not applicable

EE: エチニルエストラジオール
a): 皮下投与法では0.2 μg/kg皮下投与，経口投与法では6 μg/kg経口投与
b): 0.6 μg/kg皮下投与

下の通りであり，いずれも構造活性相関や，*in vitro*試験系の結果などからホルモン活性を有すると疑われた20物質を選択した：2-〔ビス(4-ヒドロキシフェニル)メチル〕ベンジルアルコール(CAS No. 81-92-5，東京化成工業，東京)，6-ジンゲロール（CAS No. 23513-14-6，和光純薬工業)，ロスマリン酸（CAS No. 20283-92-5，Aldrich Chemical, Milwaukee, WI)，フェノールフタレイン（CAS No. 77-09-8，シグマアルドリッチジャパン，東京)，2,2',4,4'-テトラヒドロキシベンゾフェノン（CAS No. 131-55-5，THBP，和光純薬工業)，*N*-ヘプチル4-ヒドロキシベンゾエイト（CAS No. 1085-12-7，東京化成工業)，マラカイトグリーンベース（CAS No. 510-13-4，Sigma Chemical, St. Louis, MO)，ニューフクシン（CAS No. 3248-91-7，ICN Biomedicals, Irvine, CA)，テトラゾリウムバイオレット（CAS No. 1719-71-7, Sigma Chemical, St. Louis, MO)，アルファナフトールベンゼイン（CAS No. 6948-88-5，和光純薬工業)，プラバスタチン（CAS No. 81093-37-0，和光純薬工業)，フィゾスチグミン（CAS No. 57-64-7，シグマアルドリッチジャパン)，コルヒチン（CAS No. 64-86-8，和光純薬工業)，ノルジヒドログアイアレティック酸（CAS No. 500-38-9，ICN Biomedicals, Irvine, CA)，レセルピン（CAS No. 50-55-5，和光純薬工業)，フェンブコナゾール（CAS No. 114369-43-6，ジーエルサイエンス，東京)，*o*-クレゾールフタレイン(CAS No. 596-27-0，和光純薬工業)，*N,N'*-ジフェニル-*p*-フェニレンジアミン（CAS No. 74-31-7，和光純薬工業)，1,3-ジニトロベンゼン(CAS No. 99-65-0，和光純薬工業)，ピグメントオレンジ（CAS No. 12236-62-3，国立医薬品食品衛生研究所，東京)．

本試験に先立ち，まず，投与量を設定するための毒性予備試験を実施した．すなわち，C57BL/6J系雌マウスを用いて100，300および1000 mg/kg/dayの投与群を設け，各群3匹に3日間反復投与し，死亡が認められなかった最高用量を子宮肥大試験の最高用量とした．100 mg/kg/day投与群でも死亡が認められた場合は，さらに低い用量を設定して，死亡が認められない用量を求めた．化学物質は，コーン油または注射用水で所定の濃度に調製した．群構成は，表1に従い，各物質とも公比約3とし，4用量を設定した．陰性対照群の動物には，溶媒のみを投与した．陽性対照群には，経口投与法では6 μg/kg/dayのEEを経口投与し，皮下投与法では0.2 μg/kg/dayのEEを皮下投与した．抗エストロゲン作用を調べる試験系では，経口投与法，皮下投与法のいずれの場合も，0.6 μg/kg/dayのEEを併用皮下投与した．1群当たりの匹数は6とした．子宮重量の測定およびデータの解析は，実験2と同様にした．子宮および膣は，必要に応じて病理組織学的検査を実施した．

結果

実験1：幼若マウスを用いた場合，EE投与により，経口投与法（図1A）では30 μg/kg/day以上，皮下投与法（図1B）では1 μg/kg/day以上の投与群において，子宮重量が対照群より有意に増加した．一方，卵巣摘出マウスを用いた場合，経口投与法（図2A）では10 μg/kg/day以上，皮下投与法（図2B）では0.3 μg/kg/day以上のEE投与群において，子宮重量が対照群より有意に増加した．

実験2：BPA単独投与群では，BPAの用量が増加するに従って子宮重量が増加し，100および300 mg/kg投与群で有意差が認められた（図3A)．一方，BPAとEEの併用投与群では，BPAの用量が増加するに従って子宮重量が低下し，100および300 mg/kg投与群において，有意差が認められた（図3B)．

実験3：マウスを用いて化学物質の子宮肥大試験を実施した結果，エストロゲン作用あるいは抗エストロゲン作用のいずれかを示した物質は，20物質中10物質（50%）であった（図4A)．そのうち，抗エストロゲン作用のみを示した物質は6物質（60%)，エストロゲン作用と抗エストロゲン作用の両方を示した物質は4物質（40%)，エストロゲン作用のみを示した物質はなかった(図4B)．投与経路を比較すると，経口と皮下の両方で作用がみられた物質は5物質（50%)，皮下のみが3物質（30%)，経口のみが2物質(20%）であった（図4C)．子宮重量を変化させ

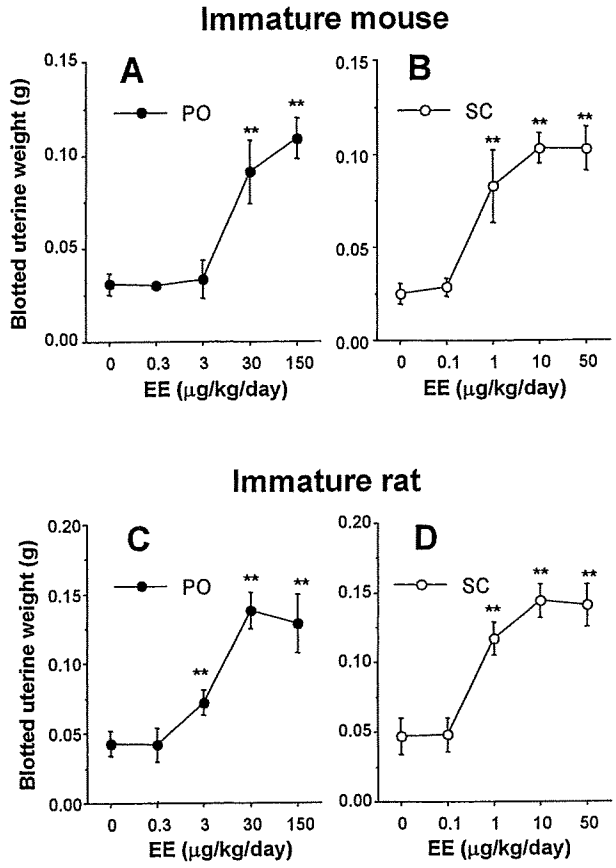

図1　幼若動物のエチニルエストラジオール（EE）投与による子宮重量増加の用量反応性

幼若動物にEEを投与し，最終投与の24時間後に測定した子宮重量（平均±標準偏差）を示す．
A：幼若マウスを用いる3日間経口投与法（PO）
B：幼若マウスを用いる3日間皮下投与法（SC）
C：幼若ラットを用いる3日間経口投与法（PO）
D：幼若ラットを用いる3日間皮下投与法（SC）
マウスの系統はICR，ラットの系統はSprague-Dawley．1群当たりの例数は5～6．
*，** は0 μg/kg群と比較して有意差（$p<0.05$, $p<0.01$）があることを示す．

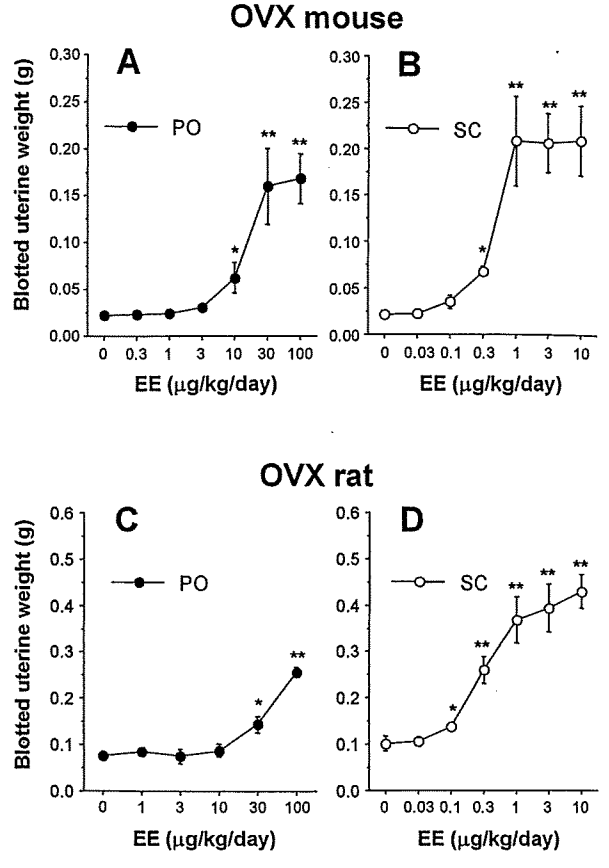

図2　卵巣摘出（OVX）動物のエチニルエストラジオール（EE）投与による子宮重量増加の用量反応性

卵巣摘出動物にEEを投与し，最終投与の24時間後に測定した子宮重量（平均±標準偏差）を示す．
A：卵巣摘出マウスを用いる7日間経口投与法（PO）
B：卵巣摘出マウスを用いる7日間皮下投与法（SC）
C：卵巣摘出ラットを用いる7日間経口投与法（PO）
D：卵巣摘出ラットを用いる7日間皮下投与法（SC）
マウスの系統はICR，ラットの系統はSprague-Dawley．1群当たりの例数は6．
*，** は0 μg/kg群と比較して有意差（$p<0.05$, $p<0.01$）があることを示す．

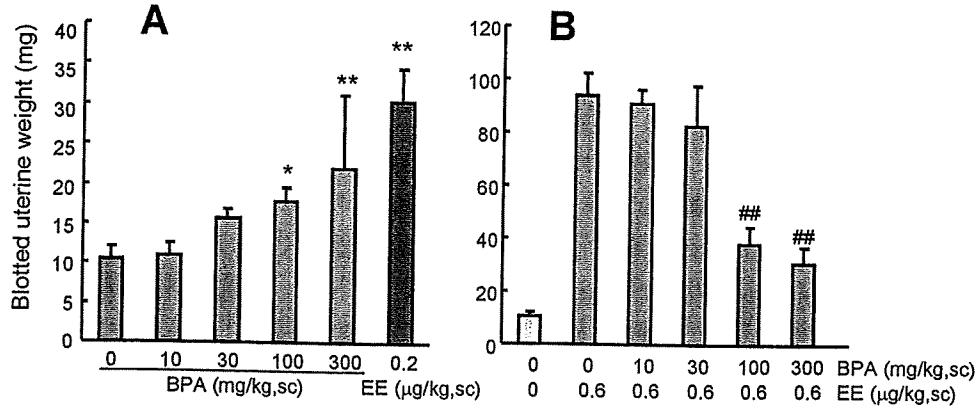

図3　ビスフェノールA（BPA）の卵巣摘出マウスを用いた子宮肥大試験

卵巣摘出マウスにBPAを7日間皮下投与し，最終投与の24時間後に測定した子宮重量（平均±標準偏差）を示す．A：エストロゲン作用を確認する試験，B：抗エストロゲン作用を確認する試験．

マウスの系統はC57BL/6J．1群当たりの例数は6．

*，** は0 mg/kg群と比較して有意差（$p<0.05$, $p<0.01$）があることを示す．

#，## は0 mg/kg BPAと0.6 μg/kg エチニルエストラジオール（EE）の併用投与群と比較して有意差（$p<0.05$, $p<0.01$）があることを示す．

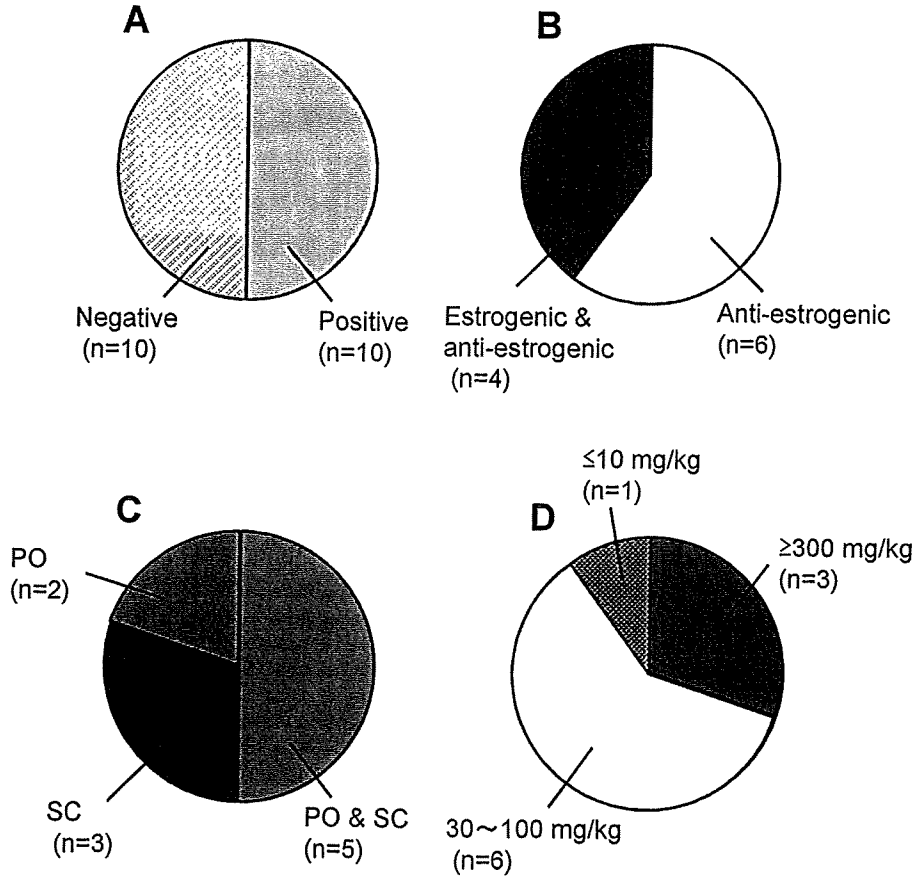

図4　化学物質の卵巣摘出マウスを用いた子宮肥大試験

卵巣摘出マウスを用いて20の化学物質について，7日間経口投与法および7日間皮下投与法で子宮肥大試験を実施し，結果を集計した．A：子宮重量に変化がみられた物質の割合，B：子宮重量に変化がみられた物質を作用別に分類，C：子宮重量に変化がみられた物質を投与別に分類，D：子宮重量に変化がみられた物質を最小有効用量で分類．

マウスの系統はC57BL/6J．POは経口投与，SCは皮下投与．

る最小有効用量は，300～1000 mg/kgが3物質（30％），30～100 mg/kgが6物質（60％），10 mg/kg以下が1物質（10％）であった（図4D）．図5には，THBPの経口投与法による子宮肥大試験の結果を示し，表2にはその時採取した子宮および膣の病理組織学的検査の結果を示した．THBP単独投与群では，1000 mg/kg投与群で子宮重量が有意に増加し（図5A），THBPとEEの併用投与群では，1000 mg/kg投与群で子宮重量が有意に低下した．病理組織像では，300 mg/kg以上の投与群で子宮内膜，腺上皮および筋層，さらには膣の粘膜上皮に陽性対照群と同様の変化がみられた．

考察

実験1のEE投与によるマウス子宮肥大試験の結果を，以前実施したSprague-Dawley系ラットを用いた子宮肥大試験[4]の結果と比較したところ，幼若動物の場合，EEに対する感度は，経口投与法ではラットの方がやや高いが（図1C），皮下投与法では差のないことがわかった（図1D）．一方，卵巣摘出動物の場合，EEに対する感度は，経口投与法ではラットの方が低く（図2C），皮下投与法ではラットの方が高いことがわかった（図2D）．エストロゲンに対する子宮の反応には，系統差がラット[5]およびマウス[6]で報告されていることから断定はできないが，今回の試験結果からは子宮肥大試験の感度にラット-マウス間の本質的な差はないと推察される．

マウス子宮肥大試験の問題点として，子宮が著しく小さいことから，重量を測定する前の脂肪除去や膣切断などに熟練を要すると考えられたが，今回の試験結果から，実体顕微鏡を用いることで，この問題点への対応は可能であると判断した．

実験2のBPA単独投与群では，用量に依存して子宮重量が増加したことから，BPAのエストロゲン作用がマウスにおいて確認された．また，今回の子宮重量を増加させる最小有効用量（100 mg/kg）は，BPAを卵巣摘出ラットに皮下投与した際の最小有効用量[4]と一致したことから，BPAに対する子宮肥大試験の感度にもラット-マウス間の差はないと推定される．一方，BPAとEEの併用投与群では，子宮重量が低下したことから，BPAの抗エストロゲン作用も確認された．これは，エストロゲン活性の弱いBPAがエストロゲン活性の強いEEの作用を阻害したものと推察されるが，実験3の化学物質の中にもエストロゲン作用と抗エストロゲン作用の両方を示す物質がみられており，山崎ら[7]も幼若ラットを用いた子宮肥大試験において，18物質中10物質にみられることを報告している．

実験3において，20の化学物質についてマウス子宮肥大試験を実施した結果，化学物質の半数に子宮重量の変化がみられたが，そのうち，エストロゲン作用のみを示した物質はなかった．このことから，化学物質の子宮肥大試験では，エストロゲン作用と抗エストロゲン作用の両方が確認できるように群構成を設定することが必要と考えられる．また，投与経路についても，約半数の物質は皮下のみ，あるいは経口のみで子宮重量に変化がみられたことから，経口と皮下の両方を実施することが望ましいと考えられる．なお，子宮重量を変化させる最小有効用量は，ほとんどが30 mg/kg以上であり，毒性が強い化学物質では，低用量から他の毒性が発現し，子宮肥大試験では変化が見えにくい傾向にあった．

マウスの子宮および膣の病理組織学的検査は，ラットに比べて標本作製が難しいと予想されたが，ホルマリン固定時に子宮を適度に伸展させたことで，標本が作製し易くなった．また，子宮重量の変化との相関も高く，ラットでみられた所見とほぼ同じ像を観察することができた．子宮および膣の組織像には明らかに系統差がみられることから，子宮肥大試験での組織観察には，種や系統間でグレード付けが異なる事態は避けられないと考えられる．しかしながら，病理組織検査は，子宮重量の変化がエストロゲン活性によるものであることを確認する重要な手段であることに変わりはないと考えられる．

本稿では，マウスを用いる子宮肥大試験の検証を目的として，EE投与によるマウス子宮重量増加の用量反応性，BPAやその他種々の化学物質について実施したマウス子宮肥大試験の結果を紹介し，マウス子宮肥大試験は，ラット子宮肥大試験と同様にエストロゲン作用や抗エストロゲン作

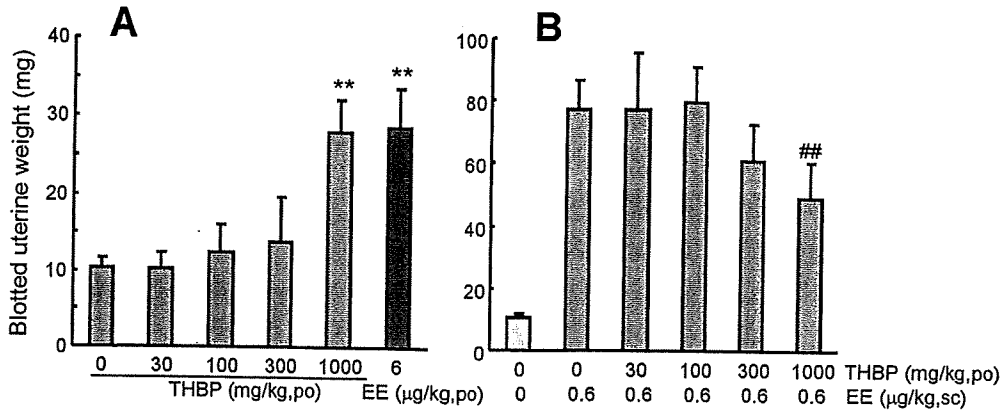

図5　2,2',4,4'-テトラヒドロキシベンゾフェノン（THBP）の経口投与法による卵巣摘出マウスを用いた子宮肥大試験

卵巣摘出マウスにTHBPを7日間経口投与し，最終投与の24時間後に測定した子宮重量（平均±標準偏差）を示す．A：エストロゲン作用を確認する試験，B：抗エストロゲン作用を確認する試験．

マウスの系統はC57BL/6J．1群当たりの例数は6．

*，** は0 mg/kg群と比較して有意差（$p<0.05$, $p<0.01$）があることを示す．

は0 mg/kg BPAと0.6 μg/kg エチニルエストラジオール（EE）の併用投与群と比較して有意差（$p<0.01$）があることを示す．

poは経口投与，scは皮下投与．

表2　2,2',4,4'-テトラヒドロキシベンゾフェノン（THBP）の子宮肥大試験における病理組織検査結果

		Estrogenic action						Antagonistic action				
	THBP (mg/kg)	0	30	100	300	1000	0	0	30	100	300	1000
Findings	EE (μg/kg)	0	0	0	0	0	6	0.6	0.6	0.6	0.6	0.6
Uterus												
Luminal epithelial cell												
Hypertrophy		-	-	-	±	±	±	++	++	++	++	+
Mitosis		-	-	-	-	+	+	±	±	±	±	±
Vacuolation		-	-	-	±	+	+	++	++	++	+	++
Glandular epithelial cell												
Hypertrophy		-	-	-	-	±	±	++	++	++	++	+
Vacuolation		-	-	-	-	+	±	±	±	±	±	±
Endometrial stroma												
Edema		-	-	-	-	-	-	±	±	±	±	-
Hypertrophy		-	-	-	±	±	±	++	++	++	++	+
Cellular infiltration, eosinophil		-	-	-	-	±	±	++	++	++	++	++
Myometrium												
Hypertrophy		-	-	-	-	±	±	++	++	++	++	++
Vagina												
Epithelium												
Cornification		-	-	-	-	±	±	+++++++++		++	+	
Thickening		-	-	-	±	+	+	+++++++++		++	+	

試験は，卵巣摘出マウスを用いる7日間経口投与法による．

マウスの系統はC57BL/6J．

エストロゲン作用のエチニルエストラジオール（EE）は経口投与，抗エストロゲン作用のEEは皮下投与．

用を有する化学物質を検出する試験系として利用できることを示した.

謝辞

最後に，本稿の連名者以外で，この研究に携わった者の氏名を掲載し，謝意を表する．野口聡，田子和美，代田眞理子，臼見憲司，加藤博康，横田俊二，関　剛幸，大澤徳子，千坂亜希子，今野和則，永田伴子，堀内伸二，稲田浩子，三枝克彦．この研究は，平成13年および14年度厚生労働省厚生労働科学研究費の補助により実施した.

文　献

1) Kanno, J., Onyon, L., Haseman, J., Fenner-Crisp, P., Ashby, J., Owens, W.: The OECD program to validate the rat uterotrophic bioassay to screen compounds for *in vivo* estrogenic responses: Phase 1. Environ. Health Perspect. **109**: 785–794 (2001)
2) Kanno, J., Onyon, L., Peddada, S., Ashby, J., Jacob, E., Owens, W.: The OECD program to validate the rat uterotrophic bioassay. Phase 2: Coded single-dose studies. Environ. Health Perspect. **111**: 1550–1558 (2003)
3) Kanno, J., Onyon, L., Peddada, S., Ashby, J., Jacob, E., Owens, W.: The OECD program to validate the rat uterotrophic bioassay. Phase 2: Dose-response studies. Environ. Health Perspect. **111**: 1530–1549 (2003)
4) 太田　亮，今井　清：ラットを用いる子宮重量試験とハーシュバーガー試験，アニテックス**13**: 24–32 (2001)
5) Diel, P., Schmidt, S., Vollmer, G., Janning, P., Upmeier, A., Michna, H., Bolt, H.M., Degen, G.H.: Comparative responses of three rat strains (DA/Han, Sprague-Dawley and Wistar) to treatment with environmental estrogens. Arch. Toxicol. **78**: 183–93 (2004)
6) Ashby, J., Owens, W., Odum, J., Tinwell, H.: The intact immature rodent uterotrophic bioassay: Possible effects on assay sensitivity of vomeronasal signals from male rodents and strain differences. Environ. Health Perspect. **111**: 1568–70 (2003)
7) Yamasaki, K., Takeyoshi, M., Sawaki, M., Imatanaka, N., Shinoda, K., Takatsuki, M.: Immature rat uterotrophic assay of 18 chemicals and Hershberger assay of 30 chemicals. Toxicology **183**: 93–115 (2003)

J. Biochem. **140**, 409–419 (2006)
doi:10.1093/jb/mvj167

AIB1 Promotes DNA Replication by JNK Repression and AKT Activation during Cellular Stress

Kikumi Horiguchi, Shigeki Arai*, Tsutomu Nishihara and Jun-ichi Nishikawa†
Laboratory of Environmental Biochemistry, Graduate School of Pharmaceutical Sciences, Osaka University, 1-6 Yamada-oka, Suita, Osaka, 565-0871

Received February 17, 2006; accepted July 19, 2006

Amplified in breast cancer 1 (AIB1) is a member of the p160 family of nuclear receptor coactivator protein. Recent studies have reported that high-level AIB1 production is involved in the phosphoinositide 3-kinase (PI3K)/Akt signaling pathway for progression to malignant carcinoma in a steroid-independent manner. Here we demonstrate that, in AIB1-knockout DT40 chicken B-lymphocytes, loss of AIB1 results in induction of phosphorylation of c-Jun N-terminal kinase (JNK) and c-Jun, in addition to the inhibition of DNA replication. In contrast, high-level AIB1 production prevents proapoptotic activation of the JNK/c-Jun signal transduction pathway and induces DNA replication through phosphorylation of the Akt/p65 NF-κB subunit RelA under cellular stresses such as UV irradiation or serum deprivation. Moreover, we have found that AIB1 is essential for the phosphorylation of histone H3 at serine 10, which is associated with the signal transduction to chromatin, leading to the transient expression of immediate-early genes in response to UV stimulation. Our results therefore suggest that AIB1 directly links to cell cycle control mechanisms in concern with the balance between apoptosis and proliferation.

Key words: amplified in breast cancer 1, cellular stress, DNA replication, phosphorylation, signal transduction.

Abbreviations: AIB1, amplified in breast cancer 1; Akt, cellular homolog of v-akt oncogene; CARM1, coactivator-associated arginine methyltransferase 1; CBP, cyclic AMP response element binding protein; CDK, cyclin dependent kinase; ER, estrogen receptor; ERK, extracellular signal–regulated kinase; FCS, fetal cauf serum; FACS, fluorence-activated cell sorting; GSK3, glycogen synthase kinase 3; HAT, histone acetyltransferase; HER-2, human epidemal growth factor receptor-2; JNK, c-Jun amino-terminal kinase; MAPK, mitosis-activated protein kinase; NF-κB, nuclear factor-κB; PAS, Per/Arnt/Sim; PI3K, phosphatidylinositol 3 kinase; RSK2, ribosomal S6 kinase 2; SRC-1, steroid receptor coactivator-1; TIF2, transcriptional intermediary factor 2; TUNEL, terminal deoxynucleotidyl transferase–mediated nick end label.

The nuclear receptor coactivator known as AIB1 (also called p/CIP, ACTR, RAC3 and SRC-3) is a member of the p160 nuclear receptor coactivator family. This family contains SRC-1 (steroid receptor coactivator-1) and TIF2 (transcriptional intermediate factor-2) that interact with the general transcriptional coactivators CBP, p300 and p/CAF (*1–8*). These coactivator complexes possess intrinsic histone acetyl transferase activity and are responsible for the remodelling of chromatin and modification of components of the transcription machinery (*9*, *10*).

AIB1 increases estrogen-dependent transcriptional activation by interaction with estrogen receptor (ER) α in a ligand-dependent manner. Furthermore, AIB1 mRNA and protein have been shown to be amplified and overexpressed in primary human breast and ovarian cancer cell lines, in which transcription is upregulated and the AIB1 gene on chromosome 20q12 is amplified (*1*). Recent studies report that high levels of AIB1 production are relates to both a high DNA-synthesis phase fraction and HER-2/*neu* production with p53 mutations in breast cancer, which is a disease characterized by an imbalance between cell division and cell death (*11*, *12*). Her-2/*neu* protein activates the PI3K (phosphoinositide 3-kinase)/Akt (also known as protein kinase B, PKB) pathway, which, through NF-κB activation, plays an important role in preventing cells from undergoing apoptosis (*13*, *14*). More recently, it has been shown that overexpression of AIB1 in the mammary gland leads to activation of the PI3K/Akt pathway, with IGF-1 signaling (*15*). Because AIB1 (RAC-3) has also been shown to interact with NF-κB and enhance its transcriptional activity (*16*, *17*), it has been suggested that AIB1 is an altered regulator for the mechanism by which constitutive activity of an NF-κB–dependent promoter is involved in chemotherapeutic resistance in ER-negative cancer cells (*18*, *19*). However, the biological function of AIB1 in the signal transduction pathways influenced by complex cascades of phosphorylation events triggered by exposure to cellular stress is not completely understood. Therefore, we focused our attention on AIB1 activity, to determine whether this protein regulates the antiapoptotic process or perturbs signal integration in response to cellular stress.

Importantly, c-Jun N-terminal kinase (JNK) has also been shown to be a key regulator of programmed cell death and part of a subfamily of the mitogen-activated protein kinase (MAPK) superfamily (*20*). Recent studies indicate that JNK activation contributes to

*Present address: Research Center for Genomic Medicine, Saitama Medical School, 1397-1 Yamane, Hidaka, Saitama 350-1241.
†To whom correspondence should be addressed. Tel: +81-6-6879-8241, Fax: +81-6-6879-8244, E-mail: nisikawa@phs.osaka-u.ac.jp

TNF-α–induced apoptosis in the absence of NF-κB activation, and that NF-κB–mediated inhibition on JNK activation is important for cell survival (*21–24*). Here we show that, in wild-type DT40 cells, high-level production of AIB1 suppresses the phosphorylation of JNK and c-Jun, the main physiological substrate of the JNK kinase, in response to cellular stress such as serum deprivation or UV irradiation. In contrast, loss of AIB1 leads to inhibition of activation of the Akt/p65 signaling pathway and suppresses DNA synthesis.

Finally, we found that AIB1 enhances the induction of phosphorylation of histone H3 at serine 10 but not the acetylation of histone H3 at lysine 9 or lysine 14 in response to UV stress. Phosphorylation of histones provides motifs for the recruitments of chromatin modifying or remodelling complexes, including coactivators which are linked to cellular processes such as transcription, DNA replication, DNA repair and apoptosis in the stress response (*25, 26*). Because AIB1 enhances the induction of phosphorylation of histone H3 at serine 10, it plays a critical role as a transcriptional modifier that is recruited for chromatin remodelling in response to cellular stresses. These results indicate that changes in AIB1 production may determine cell fate in association with the balances between the Akt/p65 and JNK/c-Jun signaling pathways in cellular stress responses.

EXPERIMENTAL PROCEDURES

Cell Culture—DT40 cell lines were maintained in RPMI 1640 (Nikkenseibutsu) medium supplemented with 10% fetal calf serum (FCS; Gibco BRL) and 1% chicken serum (JRH Bioscience) at 39.5°C in a humidified atmosphere with 5% CO_2. Cell density was maintained at 0.1–1.0/10^6 ml by splitting the culture daily.

Construction of Targeting and Expression Vectors—A chicken AIB1 (*GdAIB1*) partial cDNA fragment from the bHLH/PAS domain was amplified from chicken brain cDNA by RT-PCR with primers (5′-aaggaaaaactatttccagtgagatgatgttc-3′, 5′-cgaattgtatcctaaagccaggtctcagg-3′). We then used 5′ and 3′ RACE on chicken brain cDNA to isolate the entire open reading frame of *GdAIB1*. To construct the *GdAIB1* expression vector, chicken *AIB1* cDNA was inserted into an expression vector containing the chicken β-actin promoter. We then isolated 6.5 kb of the partial chicken genomic *GdAIB1* locus from DT40 genomic DNA by long-range PCR. Chicken *AIB1* targeting constructs were made by replacing the genomic sequence containing the sequence encoding amino acids 122 to 156 with hygromycin or histidinol selection marker cassettes.

Generation of AIB1 −/− Clones—10^7 DT40 cells were suspended in 0.5 ml PBS containing 30 μg of linearized plasmid for the transfection and electroporated with a Gene Pulser apparatus (BioRad) at 550 V and 25 μF. Following electroporation, cells were transferred into 20 ml fresh medium and incubated for 24 h. Cells were then resuspended in 80 ml medium containing hygromycin (2.5 mg/ml, Calbiochem) or L-histidinol (1 mg/ml, Calbiochem) and divided into four 96-well plates. After 7 to 10 days, drug-resistant colonies were selected. Disruption of the gene was confirmed by Southern blot analysis of genomic DNA.

Cell Cycle Analysis—A total of of 2×10^5 cells were treated with 5-bromodeoxyuridine (BrdU; 10 μM, Sigma) for 10 min and the subconfluent cells harvested. After fixation with 70% ethanol, the cells were incubated overnight at −20°C. The next day, cells were collected and resuspended in 2 N HCl with 0.5% Triton X-100 for 30 min at room temperature; this was followed by neutralization with 0.1 M $Na_2B_4O_7$. Cells were then collected and incubated with anti-BrdU antibody (Becton-Dickinson) for 30 min in the dark at room temperature. The cells were washed with PBS and stained with FITC-labeled goat anti-mouse Abs (Jackson) for 30 min at room temperature in the dark. The cells were resuspended in PBS containing propidium iodide (5 μg/ml, Sigma). The filtered cells were analyzed by fluorescence-activated cell sorter (FACScan, Becton-Dickinson). The distribution of cells in each phase of the cell cycle was determined by using Cell Quest software (Becton-Dickinson).

TUNEL Assay—DT40 cells were harvested at the designated time points and fixed in 70% ethanol in PBS. The fixed cells were then incubated for 30 min at 4°C and permeabilized with 0.2% Triton X-100 in PBS for 5 min. For apoptosis analysis, the cells were examined by the TUNEL technique, as described in the instructions supplied with the apoptosis detection system (Takara). Localized green fluorescent apoptotic cells were detected by fluorescence microscopy. The percentage of FITC-positive cells in the apoptotic fraction was determined in a fluorescence-activated cell sorter (Becton Dickinson).

Western Blot Analysis—Cells were lysed in lysis buffer (150 mM NaCl, 50 mM Tris-HCl at pH 7.5, and 1% NP-40) supplemented with protease inhibitors, aprotinin (1 μg/ml), and leupeptin (2 μg/ml). Lysates were centrifuged to clear cell debris, and then 30 μg of the total protein were size-fractionated by SDS-PAGE gel (7.5% to 15%). After electrophoresis, proteins were transferred to PVDF membranes (BioRad), blocked in PBS containing 0.2% Tween 20 and 3% bovine serum albumin, and probed with first antibody in PBS containing 0.2% Tween 20 and 1% bovine serum albumin. Detection of the immune signal was performed with the chemiluminescence detection system (Amersham Biosciences) and then quantified using densitometry (Molecular Dynamics).

Antibodies—The amino-terminal portion of chicken AIB1 (amino acids 1 to 250) was expressed in *E. coli* as a histidine tagged fusion protein and purified by affinity chromatography using Ni-agarose (Qiagen). The purified protein was then injected into rabbits to prepare specific antiserum. Rabbit antibodies of anti-phospho-Akt, anti-Akt, anti-phospho-p65, anti-p65, anti-phospho-JNK, anti-JNK, anti-phospho-c-Jun, anti-c-Jun, anti-phospho-p38, and anti-phospho-p44/42 ERK1/2 were purchased from Cell Signaling Technology. Mouse antibodies of anti-p38 and anti-ERK1 were purchased from BD Bioscience. Rabbit anti-histone H3 phosphorylated at Ser10 or Ser28 and rabbit anti-histone H3 acetylated at Lys9 or Lys14 antibodies were purchased from Upstate Biotechnology.

Immunoprecipitations and In Vitro Akt Kinase Assay—Cells were disrupted with cold RIPA buffer (50 mM Tris-HCl, pH 8.0, 150 mM NaCl, 1% NP-40, 0.5% DOC, and 0.1% SDS) containing protease inhibitors, aprotinin (1 μg/ml) and leupeptin (2 μg/ml). Approximately 200 μg of protein lysate was incubated with anti-chicken AIB1

antibody and anti-Akt antibody overnight at 4°C with end-over-end rotation, followed by an additional 2 h of incubation with protein A sepharose beads (Amersham Biosciences). The beads were then washed three times with cold RIPA buffer before being boiled in SDS-PAGE sample buffer. *In vitro* Akt kinase assay was performed for 30 min at 30°C in 40 μl of reaction volume containing 30 μl of immunoprecipitates in kinase buffer with 200 μM ATP. GSK-3 fusion protein (Cell Signaling Technology) was used as a substrate for Akt kinase activity. The reactions were terminated with 20 μl of SDS sample buffer and subjected to Western blotting using anti-phospho-GSK antibody (Cell Signaling Technology).

Northern Blot Analysis—Total RNA was isolated with Trizol reagent (Invitrogen). For generation of each probe, 1 μg of total RNA was used in reverse transcription reactions, as described by the manufacturer. The resulting total cDNA was then used in the PCR to estimate mRNA levels. The mRNA level of GAPDH was used as internal control. PCR was carried out with Taq polymerase, and the conditions were as follows: pre-denaturing at 94°C for 3 min, then 30 cycles of 94°C for 30 s, 60°C for 30 s, and 72°C for 30 s. The oligonucleotide primers used to generate these probes were as follows: AIB1 (GenBank accession number: XM417385), 5′-attacctgcattcagagaagaat-3′ and 5′-tcttctctcattgtctacacaa-3′; chicken cyclin D1 (U40844), 5′-tttacaccgacaactccatc-3′ and 5′-gtgataggaaatgtgtgagg-3′; chicken cyclin D2 (U28980), 5′-ccatcaatgatagcaactgg-3′ and 5′-aaaataaaaggggtgggag-3′; chicken cyclin E (U28981), 5′-cttcaccgctaccaattctg-3′ and 5′-caaactggtgcaactttggt-3′; chicken E2F1 (X89245), 5′-ggatccccggcagaggggca-3′ and 5′-ctccaggacattggtgatgt-3′; GAPDH (NM204305), 5′-accactgtccatgccatcac-3′ and 5′-tccacaacacggttgctgta-3′. Each total RNA (30 μg) was run on a 1.0% formaldehyde gel and transferred to a Hybond N+ nylon membrane (Amersham) using a Turbo blotter system (Schleicher & Schuell). DNA probes were labeled with [α-^{32}P] dCTP (Amersham Biosciences) using a random labeling kit (Takara). The membrane was hybridized with labeled DNA probes by QuikHyb hybridization (Stratagene) at 65°C for 2 h and then developed for autoradiography.

Histone Extraction—Cells were centrifuged, the medium discarded and the cells washed twice with PBS (pH 7.4). The cells were suspended in 5 to 10 volumes of lysis buffer (10 mM HEPES, pH 7.5, 1.5 mM $MgCl_2$, 10 mM KCl, 0.5 mM DTT and 1.5 mM PMSF). The samples were incubated on ice for 30 min and centrifuged at 1,000 × *g* for 10 min at 4°C. The supernatant was discarded, and the histones in the pellets were extracted by 0.2 M HCl solution. The samples were centrifuged at 12,000 × *g* for 10 min at 4°C after incubation on ice for 30 min. The histones were then precipitated from acid solution with 5 volumes of cold acetone.

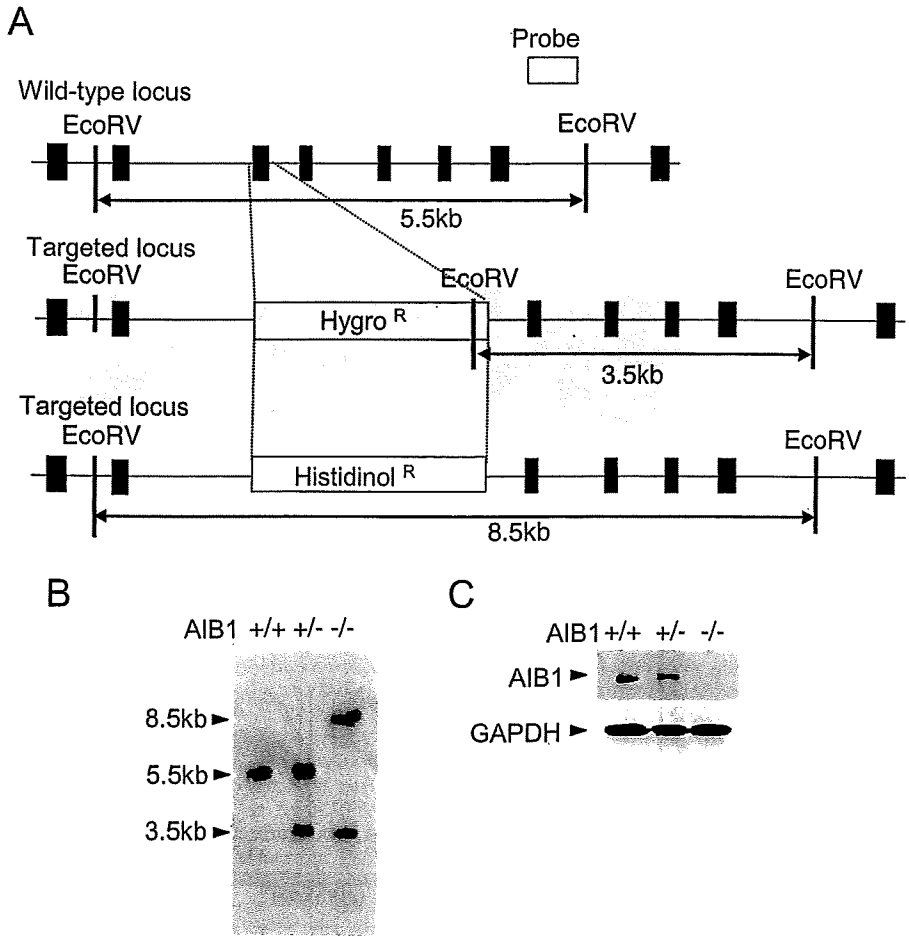

Fig. 1. **Generation of AIB1-knockout DT40 cells.** (A) Schematic representation of the targeting vectors. The configuration of the wild-type allele is shown at the top. In the targeting vectors, the exon encoding the Per-Arnt-Sim (PAS) domain is replaced by a hygromycin or histidinol resistance gene cassette. Solid boxes indicate positions of exons deduced from the cDNA sequence. The location of the external probe used to confirm correct targeted events and the location of the relevant *EcoRV* recognition sites are indicated. (B) Southern blot analysis of targeted integration. A DT40 cell in which one *AIB1* allele had been disrupted by the targeting construct of AIB1-hygromycin, was transfected with the second construct of AIB1-Histidinol. Genomic DNAs from untransfected DT40 cells (+/+) and doubly resistant clones (–/–) were digested with *EcoRV* and hybridized with the probe shown in (A). (C) Western blot analysis of wild-type, AIB1$^{+/-}$ and AIB1$^{-/-}$ DT40 cells. GAPDH protein was detected as an internal control.

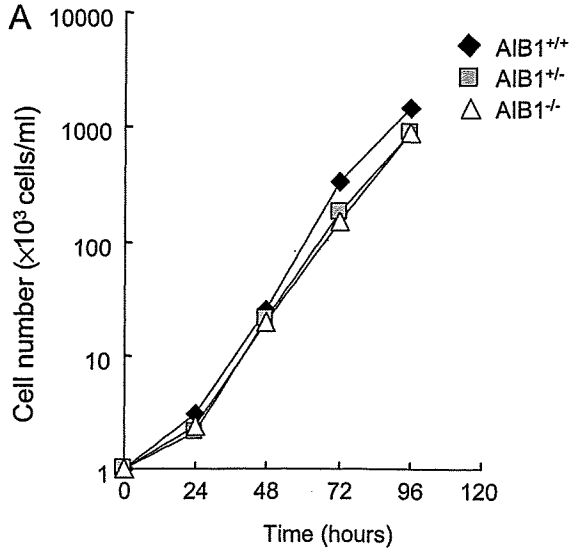
A
Cell number (×10³ cells/ml)
10000
1000
100
10
1
0 24 48 72 96 120
Time (hours)
AIB1+/+
AIB1+/-
AIB1-/-

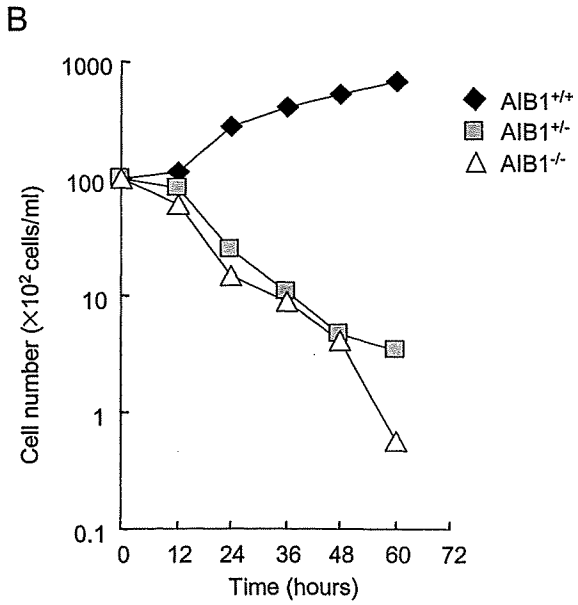
B
Cell number (×10² cells/ml)
1000
100
10
1
0.1
0 12 24 36 48 60 72
Time (hours)
AIB1+/+
AIB1+/-
AIB1-/-

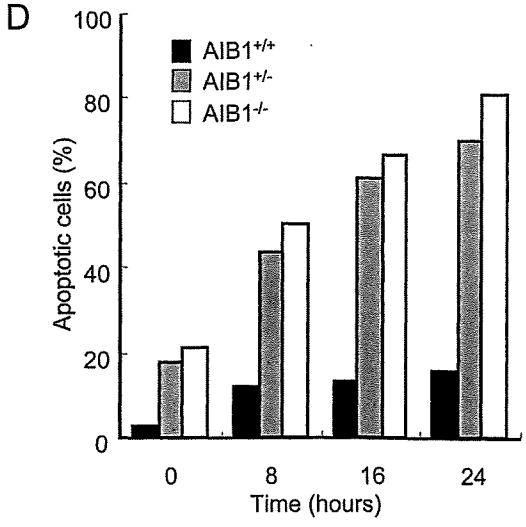
D
Apoptotic cells (%)
100
80
60
40
20
0
0 8 16 24
Time (hours)
AIB1+/+
AIB1+/-
AIB1-/-

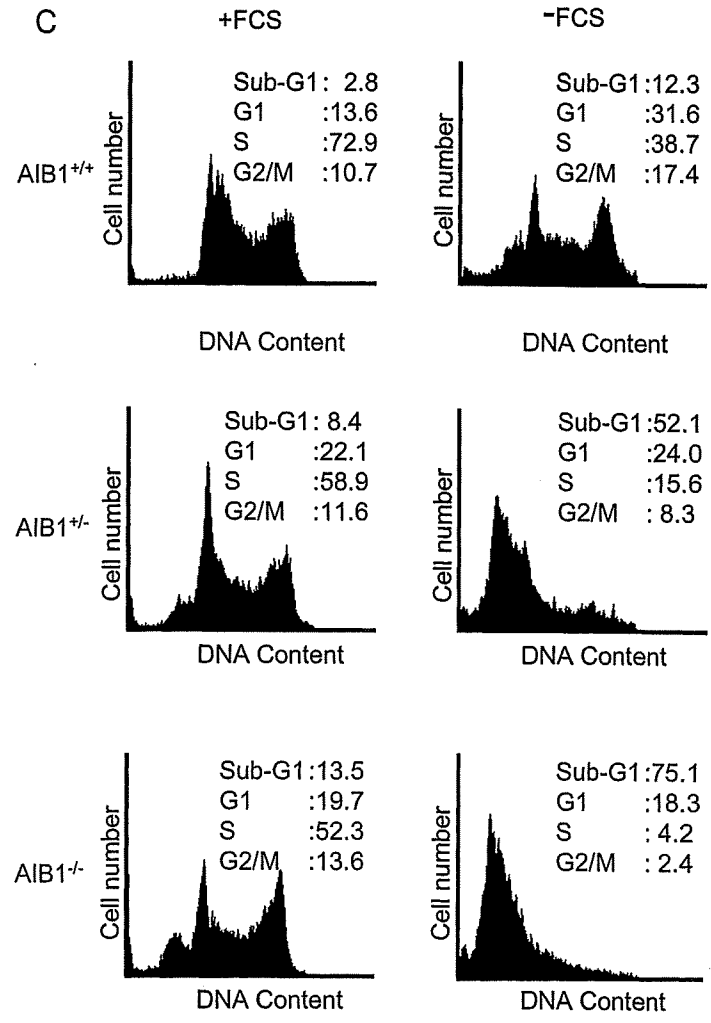
C
+FCS
-FCS
AIB1+/+
AIB1+/-
AIB1-/-
Cell number
Sub-G1: 2.8
G1 :13.6
S :72.9
G2/M :10.7
Sub-G1:12.3
G1 :31.6
S :38.7
G2/M :17.4
Sub-G1: 8.4
G1 :22.1
S :58.9
G2/M :11.6
Sub-G1:52.1
G1 :24.0
S :15.6
G2/M : 8.3
Sub-G1:13.5
G1 :19.7
S :52.3
G2/M :13.6
Sub-G1:75.1
G1 :18.3
S : 4.2
G2/M : 2.4
DNA Content

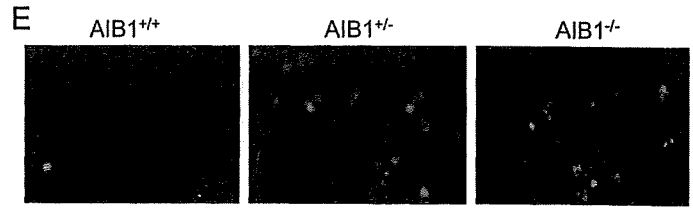
E
AIB1+/+
AIB1+/-
AIB1-/-

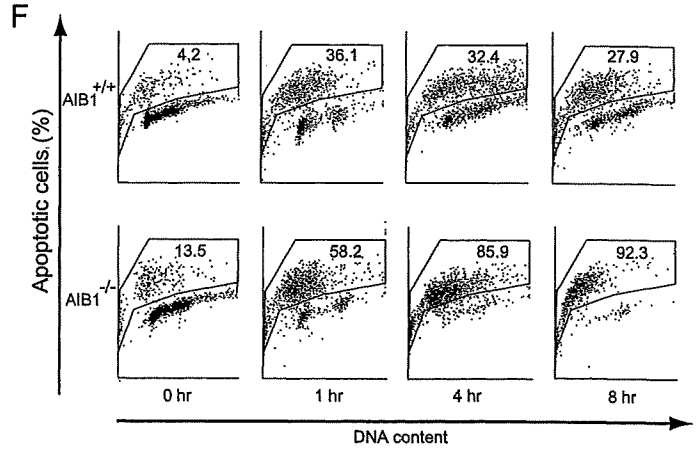
F
Apoptotic cells (%)
AIB1+/+
AIB1-/-
4.2
36.1
32.4
27.9
13.5
58.2
85.9
92.3
0 hr
1 hr
4 hr
8 hr
DNA content

RESULTS

Generation of AIB1-Knockout DT40 Cells—To investigate the biological function of AIB1 in the signal transduction pathways triggered by cellular stress, we generated a model for the elimination of AIB1 production by using DT40 B-lymphocytes that constitutively express high levels of *c-myc* as a result of transformation by an avian leukosis virus (*27*). Because of their high rate of homologous recombination in vertebrate cells, DT40 cell lines have also been used as models for establishing strategies to identify genes that encode undiscovered components of a process or a pathway (*28*). We previously reported the cloning of a chicken homologue of AIB1 that exhibits 74.4% amino acid sequence similarity to human AIB1 (*29*). A full-length transcript of the gene encoding chicken AIB1 was isolated and found to encode a 1,399–amino acid protein. An AIB1 deletion construct was generated (Fig. 1A) and a portion of the AIB1 genomic locus was replaced with a hygromycin resistance gene and a histidinol resistance gene. The targeted homologous recombination in DT40 cells was confirmed by Southern blot analysis of genomic DNA (Fig. 1B). The deleted region encoded amino acid residues 122 to 156, including the PAS domain. AIB1-knockout DT40 cells were detected by Western blot analysis using anti-AIB1 antibody (Fig. 1C).

AIB1 Promotes Cell Survival in Response to Cellular Stress in DT40 Cells—To determine the roles of AIB1 in mechanisms mediated by exposure to cellular stress in cancer cells, we examined whether loss of AIB1 was associated with changes in the regulatory mechanism of cell proliferation and cell death. Under standard culture conditions, we detected no significant difference in the rates of cell proliferation of wild-type and AIB1-knockout DT40 cells (Fig. 2A). However, AIB1-knockout cells were more susceptible to cell death than were wild-type cells in response to cellular stresses such as serum starvation. Usually, DT40 cells were maintained in medium with 10% FCS and 1% chicken serum. After deprivation of FCS, survival number of AIB1-knockout cells rapidly decreased in contrast with wild type cell (Fig. 2B). The heterozygote also manifested considerable decrease in cell number, suggesting that gene dosage of AIB1 is crucial for cell survival under serum starvation (Fig. 2B). FACS analysis revealed that 75.1% of the AIB1-knockout cells were in the sub-G1 fraction (reflecting cell death), as compared to 12.3% for the wild-type cells under serum starvation (Fig. 2C). In contrast, the S-fraction (indicating DNA synthesis) was greater in wild-type cells than in AIB1-knockout cells (Fig. 2C). In order to confirm that these cell death were apoptosis, we carried out TUNEL analysis. When cells were stained by the TUNEL after deprivation of FCS, the double-stained cells (reflecting apoptosis) increased much more in $AIB1^{+/-}$ and $AIB1^{-/-}$ DT40 cells than in wild-type DT40 cells (Fig. 2, D, E). We observed similar results in the responses to not only serum starvation but also other forms of cellular stress, such as UV irradiation (10 J/m^2) (Fig. 2F) and culture at low temperature (data not shown). These results revealed that loss of AIB1 increased apoptosis in AIB1-knockout cells under cellular stress conditions.

Deletion of AIB1 Enhances Stress-Induced JNK/c-Jun Activation and Prevents Akt/p65 Activation—Signal cascades in response to cell survival have been linked to cancer and inflammatory disease. Previous studies have shown that cellular responses are regulated by the signaling pathways that lie downstream of the Ras induced by cross talk between the Raf-MER-ERK and PI3K-Akt pathways in breast cancer cells (*21*, *22*). Moreover, the PI3K/Akt/NF-κB pathway plays an important role in preventing cells from undergoing apoptosis and contributes to the pathogenesis of malignancy (*23*). Recently, cell proliferation and survival were reported to require activation of the PI3K/Akt pathway, which has been implicated in the control of Myc protein stability (*24*). The most recent study in transgenic mice also implicated overexpression of the *AIB1* gene in the etiology of breast cancer (*15*). However, these findings and our results in Fig. 2 raise the possibility that increased AIB1 production serves to promote cell survival through the PI3K/Akt pathway in response to cellular stress. Cell survival in response to stressful stimuli has been implicated in the activation of many signal transduction pathways, such as the p38 mitogen-activated protein kinase (MAPK) pathway, the stress-activated JNK pathway, and the PI3K/Akt pathway (*30–32*). Therefore, we investigated how signal pathways might be involved in AIB1-mediated cell survival in response to cellular stress. For Western blot analysis, wild-type and AIB1-knockout DT40 cells were cultured under normal conditions or cellular stress conditions. At first, stressful stimuli such as serum starvation or UV irradiation induced phosphorylation of NF-κB subunit p65 and Akt in wild-type DT40 cells (Fig. 3A). In contrast, phosphorylation of p65 and Akt were abolished in AIB1-knockout cells (Fig. 3A). To confirm the Akt activation under stress conditions, Akt activity was detected by an

Fig. 2. **AIB1 promotes cell survival in response to serum starvation and UV irradiation.** (A) Growth curves of wild-type, $AIB1^{+/-}$ and $AIB1^{-/-}$ DT40 cells under standard conditions. Cells were cultured in RPM1640 medium supplemented with 10% fetal calf serum (FCS) and 1% chicken serum at 39.5'C. Representative growth curves correspond to the indicated cell cultures. The number of cells was counted every 24 h by FACS with polybeads as the internal standard. Each experiment was conducted three times, and each time point was determined in triplicate. (B) AIB1 was required for cell survival under serum-starved conditions. Cells were cultured at 39.5°C in fresh RPM1640 medium supplemented with 1% chicken serum, after being maintained continuously with 10% FCS and 1% chicken serum. The number of cells was counted every 12 h. (C) Cell cycle analyses of wild-type, $AIB1^{+/-}$, and $AIB1^{-/-}$ DT40 cells in the presence or absence of FCS over 24 h. The DNA content of the cultured cells was examined by propidium iodide staining. The populations of the sub-G1, G1, S, and G2/M fractions are indicated by percentages. (D) Wild-type DT40 cells were inhibited from undergoing apoptosis under serum starvation, as measured by TUNEL analysis. Cells were cultured in the absence of FCS for the periods indicated. The cells were then stained for TUNEL analysis. Double-stained cells were counted as apoptotic and are shown as the percentages in three independent experiments. (E) DNA breaks, characteristic of apoptosis, were detected under fluorescent microscope by TUNEL analysis. Cells were harvested after being cultured for 8 h in the absence of FCS. (F) DNA replication was induced in wild-type DT40 cells under the stimulation of UV-irradiation, as measured by TUNEL analysis. After UV-irradiation (10 J/m^2) the cells were cultured for the periods indicated and then stained for TUNEL analysis. Double-stained cells were counted as apoptotic and are shown as percentages from three independent experiments.

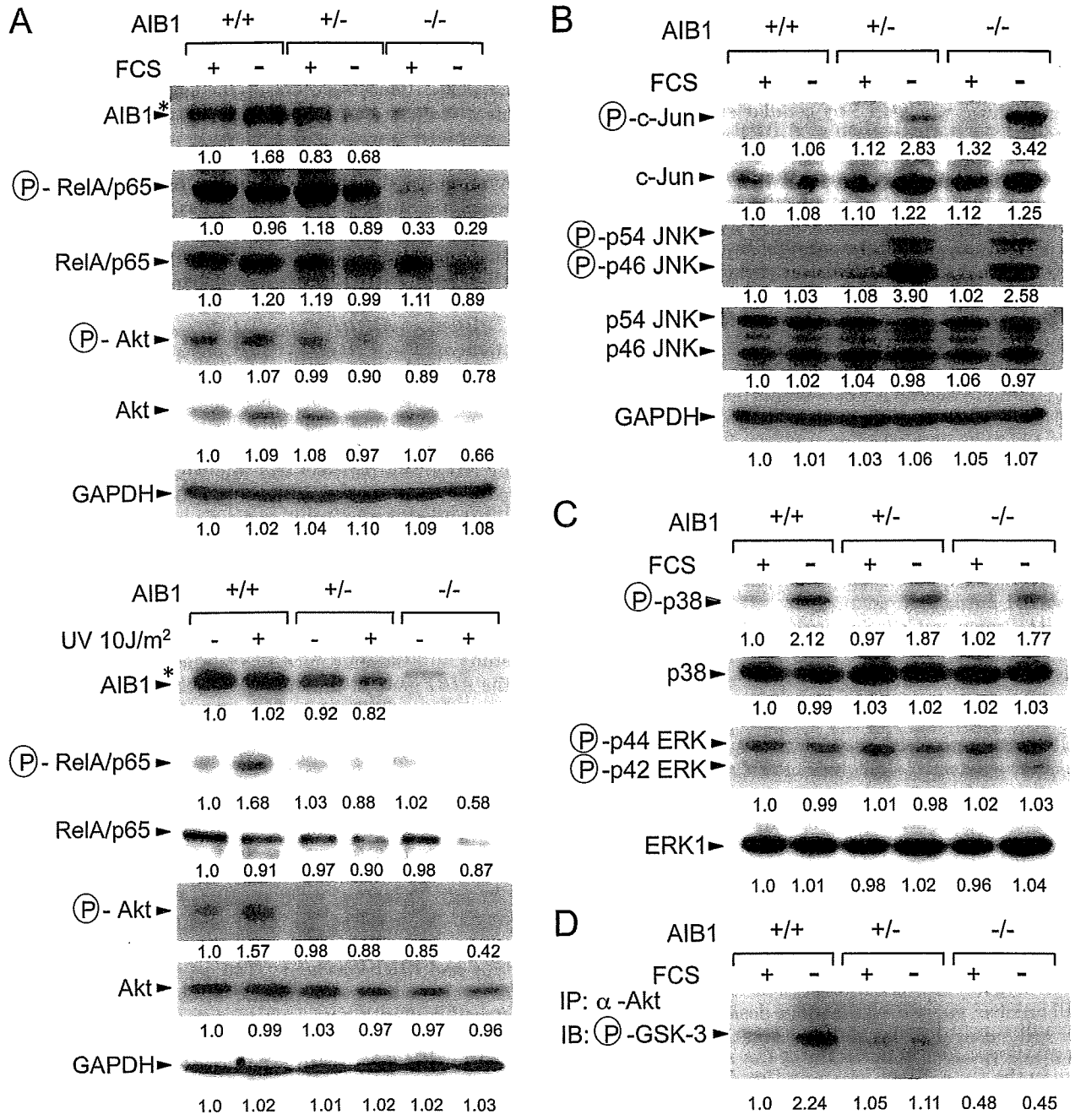

Fig. 3. **Activation of AIB1 triggers Akt survival pathway and blocks JNK-mediated cell death.** (A) Serum starvation and UV irradiation of wild-type DT40 cells induced Akt and p65 phosphorylation. The levels of production of proteins and phosphoproteins in the Akt/NF-κB cell-survival pathway were indicated by immunoblot analysis using 30 μg cell extracts prepared from wild-type, AIB1$^{+/-}$, or AIB1$^{-/-}$ DT40 cells cultured for 8 h in the presetnce or absence of FCS, with or without stimulation of UV-irradiation (10 J/m^2). The "P" in the circles indicates phosphorylation. The asterisk indicates that AIB1 antibody cross-reacted with the unspecific cytoplasmic protein. (B) Phosphorylation of JNK and c-Jun were induced by serum starvation in AIB1-knockout cells. The levels of production of protein and phosphoprotein in the JNK-mediated apoptosis pathway are indicated as shown in (A). (C) The presence of AIB1 protein did not affect the activation of the ERK or p38 MAPK pathways. (D) Serum starvation of wild-type DT40 cells induced Akt kinase activity. *In vitro* kinase assay was performed with immunoprecipitated Akt. Akt kinase activity is indicated by immunoblot analysis with glycogen synthase kinase-3 as a substrate. Western blots were quantified by densitometry and relative intensities of each band are shown.

in vitro assay of Akt-catalyzed phosphorylation of GSK3 (Fig. 3D). The catalytic activity of Akt was increased in wild-type DT40 cells by serum starvation. The activation of the PI3K/Akt pathway might be related to the cell survival of wild-type DT40 cells under stress conditions.

Second, serum starvation induced phosphorylation of c-Jun and JNK in AIB1-deficient cells, not in wild type cells (Fig. 3B). Because both of AIB1$^{+/-}$ and AIB1$^{-/-}$ cells were killed by FCS deprivation (Fig. 2B), there are good correlation between the activation of JNK/c-Jun pathway

and the cell death. The stress-activated JNK pathway might be related to the cell death of AIB1-deficient cells under stress condition. On the other hand, there was no difference in the p38 MAPK/ERK pathway (Fig. 3C). Taken together, our data suggest that AIB1 acts as a molecular link between Akt/p65-induced cell survival and JNK/c-Jun-regulated cell death in response to cellular stress.

In Fig. 3A, a band was observed in the panel for $AIB1^{-/-}$ cells. This weak signal was found in all lanes using anti-AIB1 antibody, although it was difficult to identify because it was just above the specific band. Possibly, our AIB1-antibody might cross-react to the closely related protein such as TIF2 or SRC1.

Cellular Stress Induces Upregulation of AIB1 Gene Expression—To test directly whether cellular stress causes increased AIB1 gene expression by modulating Akt function or cell cycle regulators in GI/S transition, we examined the levels of expression of the mRNAs of various cell cycle regulators by Northern blotting in wild-type or AIB1-knockout DT40 cells after stimulation by serum starvation (Fig. 4). The mRNA levels of all the regulators investigated in AIB1-knockout cells were decreased efficiently by serum starvation. In contrast, the mRNA levels of AIB1, Akt, and RSK2 in wild-type DT40 cells were increased significantly by serum deprivation. No notable increases in mRNA levels of the G1/S-cell cycle regulators cyclin D1, cyclin D2, cyclin E and E2F1 were found in wild-type DT40 cells under serum starvation. These data indicate that, under cellular stresses such as serum starvation, high levels of AIB1 mRNA are mediated by Akt or RSK2, but not by activation of the regulators of cell cycle progression in the G1/S phase. Accordingly, cellular stress-induced AIB1 amplification may enhance cell survival and DNA replication through coordinated upregulation of the Akt signaling pathway.

AIB1 Is Essential for Induction of Akt-Dependent DNA Replication in Response to Cellular Stress—To assess the role of AIB1 in mediating Akt-activated DNA replication in response to cellular stress, we analyzed the contribution of phosphorylated Akt at designated time points after synchronization of the cell cycle by treatment with hydroxyurea, which arrests the cycle in the early S-phase. While we observed no differences in the low levels of Akt phosphorylation during synchronization, phosphorylation of Akt was blocked in AIB1-knockout DT40 cells, unlike in wild-type cells, after release of the cell cycle arrest. In contrast, induction of Akt phosphorylation was significantly increased in wild-type cells when they were released from arrest and progressed further into S phase (Fig. 5A). By treatment with the pharmacological agent LY294002, an inhibitor of PI3K/Akt kinase, we next investigated whether the requirement for AIB1 in DNA replication was dependent on Akt in stressed cells. Wild-type DT40 cells with LY294002 had marked decreased numbers of BrdU-positive cells (Fig. 5B), suggesting that, in wild-type cells, inhibition of cell cycle progression into S phase occurred by the inhibition of Akt, in the same way as in AIB1-knockout cells. Inhibition of MAPK activity by treatment with PD98059 did not lead to a marked decrease in DNA replication in response to serum starvation in wild-type DT40 cells (data not shown). Thus, these results indicate that induction of Akt phosphorylation as a consequence of progression into S phase caused a requirement for AIB1 in DNA replication in response to cellular stress.

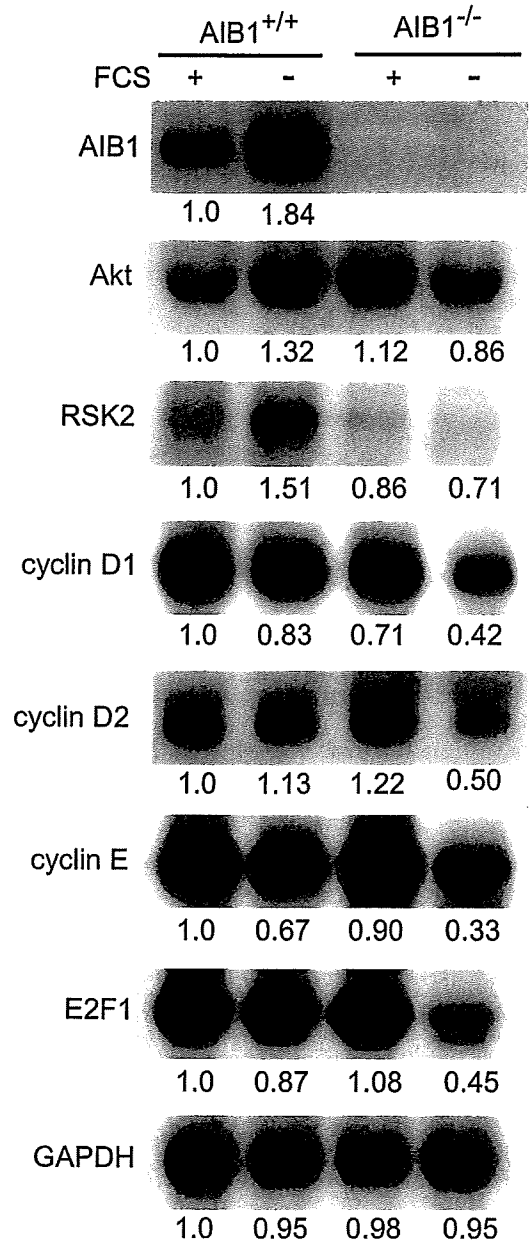

Fig. 4. **Relative levels of expression of mRNAs of cell cycle regulators.** Wild-type and AIB1-knockout DT40 cells were cultured for 8 h in the presence or absence of FCS. Total RNAs were prepared for Northern blot analysis. The radioactivities of the corresponding bands of cell cycle regulators and GAPDH mRNA were determined with an image analyzer as relative intensity, and the normalized intensity against levels of mRNA in wild-type DT40 cells with FCS are shown.

Recent study showed that AIB1 overexpression enhanced the activation of PI3K/Akt pathway and AIB1 knockdown increased apoptosis (*15*). As mentioned above, the stress-activated JNK pathway was suppressed in the presence of AIB1 (Fig. 3B). In order to investigate if the JNK suppression is mediated by the PI3K/Akt pathway, we

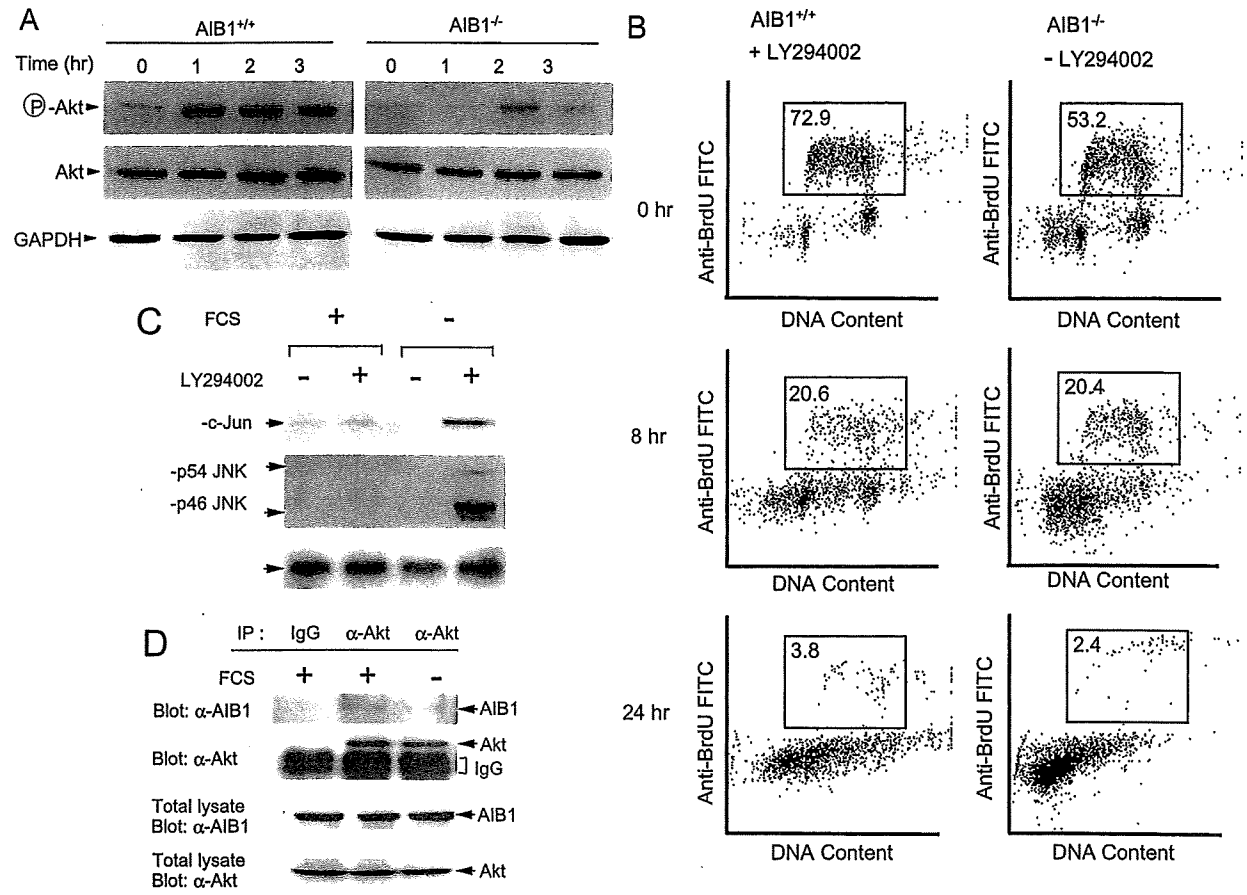

Fig. 5. **Inhibition of Akt or deficiency of AIB1 blocks DNA replication under stress conditions.** (A) Akt phosphorylation and AIB1 production were required for DNA replication. Cells were synchronized for 8 h with hydroxyurea (1 mM), which interfered with cell cycle progression by preventing DNA replication, and were harvested at the indicated points (0–3 h) following release from the cell cycle arrest. Production of phosphorylated Akt and total Akt was determined by immunoblot analysis using anti-phospho-Akt (Ser-473) and anti-Akt antibodies. (B) DNA replication in wild-type DT40 cells by in response to serum deprivation was blocked by LY294002, an inhibitor of PI3K/Akt. Wild-type cells or AIB1-knockout cells were cultured with LY294002 (50 μM) in the absence of FCS for 8 h or 24 h. The percentage BrdU positivity was determined by counting the number of cells at the BrdU-positive gates. (C) The JNK suppression in the AIB1-positive cells was blocked by LY294002. Wild-type cells were cultured with or without LY294002 (50 μM) in the presence or absence of FCS for 8 h. The levels of phosphoprotein in the JNK-mediated apoptosis pathway were determined by Western blot. (D) AIB1 is physically associated with Akt. The DT40 cell extracts were immunoprecipitated with anti-Akt antibody. For control, cell extract was precipitated with the IgG from non-immunized rabbit. The immunoprecipitates (IP) were subjected to Western blot analysis with the indicated antibodies.

examined the phosphorylation of c-Jun and JNK after LY294002 treatment. As a result, we found the marked increase of phospho-c-Jun and phospho-JNK by the LY294002 treatment in response to serum starvation (Fig. 5C), suggesting that the inhibition of PI3K/Akt pathway blocked the AIB1-mediated JNK suppression. Further, we showed the direct interaction between AIB1 and Akt (Fig. 5D). Collectively, these data suggested that AIB1 might be activated by Akt.

Loss of AIB1 Leads to Inhibition of UV-Induced Phosphorylation of Histone H3 at Serine 10—DNA replication is linked to chromatin modulation. This is associated with the modification of chromatin-associated proteins such as histones (H2A, H2B, H3, and H4) or remodeling cofactors, which are known to possess intrinsic histone acetyltransferase activity and are capable of chromatin modification by histone acetylation (*9*, *10*). We have shown here that AIB1 depletion causes a marked defect in the ability to induce DNA replication in response to cellular stress. Therefore, AIB1 may control the signal cascades for the remodeling of chromatin in response to cellular stress. We next examined whether AIB1 was required for phosphorylation of chromatin modulation in response to cellular stress. By Western blot analyses using cell extracts of acid-soluble proteins, we found that wild-type cells had a marked increase in the phosphorylation of histone H3 at serine 10 (Fig. 6), but not in the acetylation of histone H3 at lysine 9 or 14 (data not shown), very soon after treatment with UV-irradiation. This phosphorylation was completely eliminated under stress conditions by the loss of AIB1 in AIB1-knockout cells (Fig. 6). Although a previous study had shown that AIB1 possesses intrinsic histone acetyltransferase (HAT) activity for chromatin modification (*2*), we observed no difference in the levels of acetylation of histone H3 at lysine 9 and lysine 14 in AIB1-knockout DT40 cells compared with wild-type cells